



HAL
open science

Air-Stable Bis-Cyclometallated Iridium Catalysts for Ortho-Directed C(sp²)-H Borylation

Janis M Zakis, Antonis M Messinis, Lutz Ackermann, Tomas Smejkal, Joanna
Wencel-delord

► **To cite this version:**

Janis M Zakis, Antonis M Messinis, Lutz Ackermann, Tomas Smejkal, Joanna Wencel-delord. Air-Stable Bis-Cyclometallated Iridium Catalysts for Ortho-Directed C(sp²)-H Borylation. *Advanced Synthesis and Catalysis*, 2024, 366 (10), pp.2292-2304. 10.1002/adsc.202301411 . hal-04857913

HAL Id: hal-04857913

<https://hal.science/hal-04857913v1>

Submitted on 28 Dec 2024

HAL is a multi-disciplinary open access archive for the deposit and dissemination of scientific research documents, whether they are published or not. The documents may come from teaching and research institutions in France or abroad, or from public or private research centers.

L'archive ouverte pluridisciplinaire **HAL**, est destinée au dépôt et à la diffusion de documents scientifiques de niveau recherche, publiés ou non, émanant des établissements d'enseignement et de recherche français ou étrangers, des laboratoires publics ou privés.

Air-Stable Bis-Cyclometallated Iridium Catalysts for Ortho-Directed C(sp²)-H Borylation

Janis M. Zakis,^{a, d} Antonis M. Messinis,^b Lutz Ackermann,^{b, c} Tomas Smejkal,^a and Joanna Wencel-Delord^{d, e,*}

^a Automation Chemistry Research, Syngenta Crop Protection AG, Schaffhauserstrasse 101, Stein AG 4332, Switzerland

^b Institut für Organische und Biomolekulare Chemie, Georg-August-Universität Göttingen, Tammannstraße 2, 37077 Göttingen, Germany

^c Wöhler-Research Institute for Sustainable Chemistry (WISCh), Georg-August-Universität Göttingen, Tammannstraße 2, 37077 Göttingen, Germany

^d Laboratoire d'Innovation Moléculaire et Applications (UMR CNRS 7042), Université de Strasbourg/Université de Haute-Alsace, ECPM, Strasbourg 67087, France

^e Institut für Organische Chemie, Universität Würzburg, Am Hubland, 97074 Würzburg, Germany
E-mail: wenceldelord@unistra.fr

Abstract: We report a class of isolable bis-cyclometallated iridium precatalysts (ImIr) and their use in regioselective *ortho*-C–H borylation of aromatic, heteroaromatic, acrylic, and aliphatic systems. The catalysts consist of two imine ligands and an acetate coordinated to an iridium (III) center. The isolable character of ImIr warrants its compatibility with high-throughput experimentation, a prerequisite for applications in late-stage functionalization (LSF) of complex substrates. Initial mechanistic studies point towards an inner-sphere mechanism involving bis-cyclometallated species shedding light on the general mechanistic understanding of *ortho*-selective C–H borylations.

Keywords: Metallacycle; C–H activation; Ortho-directed; Borylation; Imine ligand

Introduction

Over the last two decades, C–H bond activation has transitioned from an academic curiosity to a practical methodology with applications in drug synthesis.^[1] Among the diversity of bond-forming reactions possible via C–H activation, C–H borylation has been established as a particularly attractive transformation due to the synthetic versatility of the resulting C–B bond.^[2] Various rhodium,^[3] cobalt,^[4] and ruthenium^[5] based catalytic systems have been designed. However, iridium-catalyzed C–H borylation remains the most effective and frequently used.^[6] The initial reports spearheaded by Hartwig, Miyaura, Ishiyama (Figure 1a), as well as Smith focused on undirected C–H borylations allowing functionalization of the most

sterically accessible and/or electronically favored C–H bond.^[6b,7] More recently, directed C–H borylations have emerged, in which a coordinating motif (directing group DG) governs the regioselectivity of the direct C–B coupling.^[6c,8] The combination of a precisely designed DG preinstalled on the substrate with an appropriate ligand and an Ir-based precatalyst has led to complementary strategies towards *ortho*-, *meta*- and *para*-selective direct borylations of aromatic and heteroaromatic substrates.^[6c]

The pioneering work of Hartwig illustrated the potential of silane DG (Figure 1b, **B**) in combination with bipyridine-type ligands to favor the desired *ortho*-borylation.^[9] Subsequently, multiple groups have reported *ortho*-directed C–H borylation using various catalytic systems including mainly phosphine

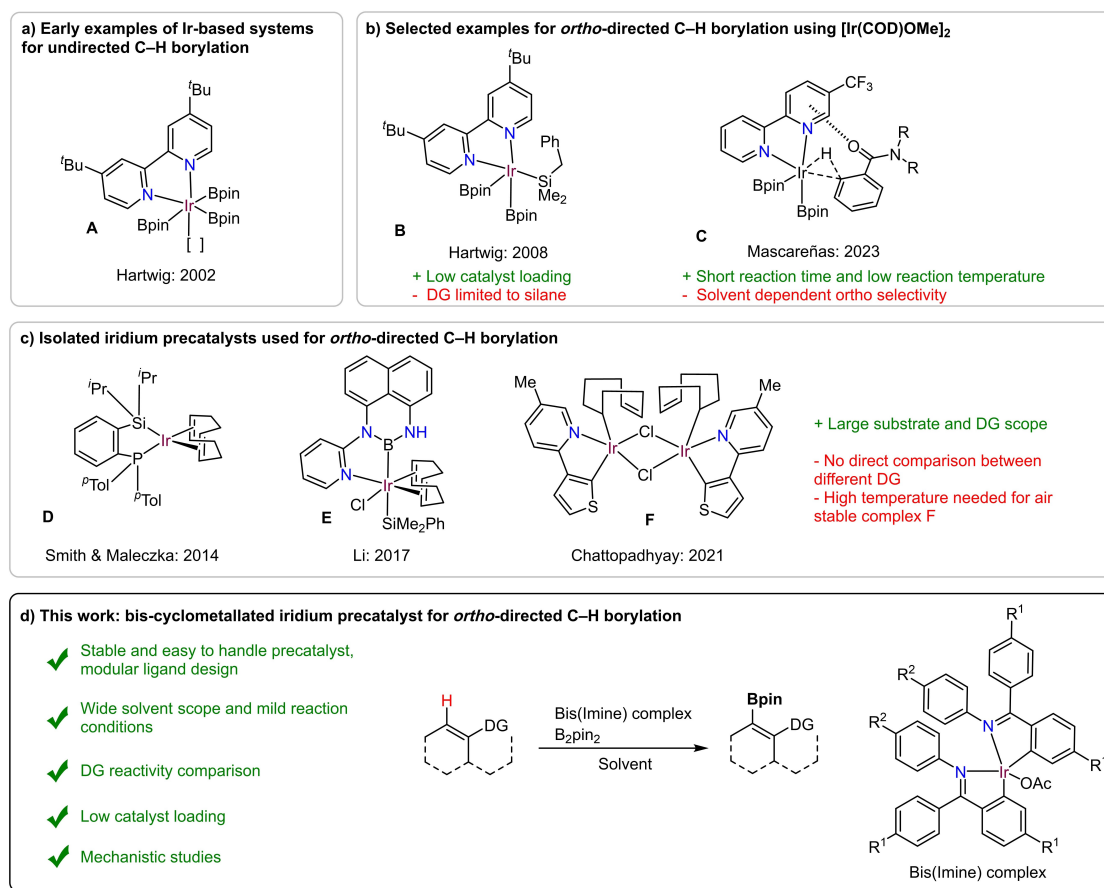


Figure 1. Iridium-catalyzed *ortho*-directed C–H borylation.

ligands^[10] and *N,N*-ligands (Figure 1b, C).^[11] Several reports have also proposed metallacyclic intermediates as key active catalyst species.^[11d,e,12] Despite the efficiency of such systems further improvements are desired such as, expanding of the DG scope, circumventing a need of a substrate's excess, and replacement of the air and water-sensitive Ir complex – $[\text{Ir}(\text{COD})\text{OMe}]_2$.^[13]

The chemistry of metallacycles has attracted scientific curiosity for decades.^[14] Pioneering efforts of organometallic chemists were devoted to synthesizing such compounds via stoichiometric reactions between an organic molecule and a metal precursor,^[14a–d] thus providing a basis for the later development of catalytic C–H activation reactions.^[15] Over the last few years, various pallada-, ruthena-, and irida-cyclic species have been synthesized, and their catalytic activity has been confirmed in various direct functionalization reactions.^[16] Based on these observations, the use of metallacyclic species as isolable catalysts for challenging C–H activation reactions has emerged, providing not only more reactive systems but also allowing the design of novel C–H activation reactions.^[15d,17]

Over the years, diversity of iridium precatalysts has shown their capacity to induce the *ortho*-directed C–H borylation (Figure 1c, D, E).^[10c,18] More recently, Chattopadhyay reported for the first time the potential of metallacyclic iridium(I) and iridium(III) precatalysts containing the 2-thienylpyridine (C,N-ligand) for C–H borylation (Figure 1c, F).^[19] However, the air-stable complex **F** requires an elevated reaction temperature (up to 120 °C in THF) and an increased B_2pin_2 loading to promote the desired C–H functionalization efficiently, thus rendering this catalytic system inadequate for the high-throughput experimentations (HTE). Indeed, the reaction discovery via HTE approach requires use of stable and easy to handle catalysts, to avoid experimental difficulties while operating. Therefore, intrigued by the reactivity of metallacyclic species as catalysts in C–H activation reactions, we hypothesized that the careful design of alternative C,N ligands could allow for the preparation of more catalytically active, air-stable and well-defined iridium complexes for direct borylations. Such an air-stable single component catalyst would prevent multicomponent weighing of air and water-sensitive materials and avoid solvent dependence of the catalyst preformation

process. Additionally, the use of well-defined metal-lacyclic catalysts may aid fundamental mechanistic understanding of other *in situ* formed catalytic systems.

Herein we report the development of air-stable bis-cyclometallated iridium(III) precatalysts and their use in *ortho*-directed borylation of aromatic, heteroaromatic, acrylic C–H bonds, as well as a selected example of C(*sp*³)–H borylation. The precatalysts are formed from iridium acetate and bear two imine ligands, one of which gets released during the precatalyst activation.

Results and Discussion

C,N Ligand Screening and Cyclometallated Catalyst Studies

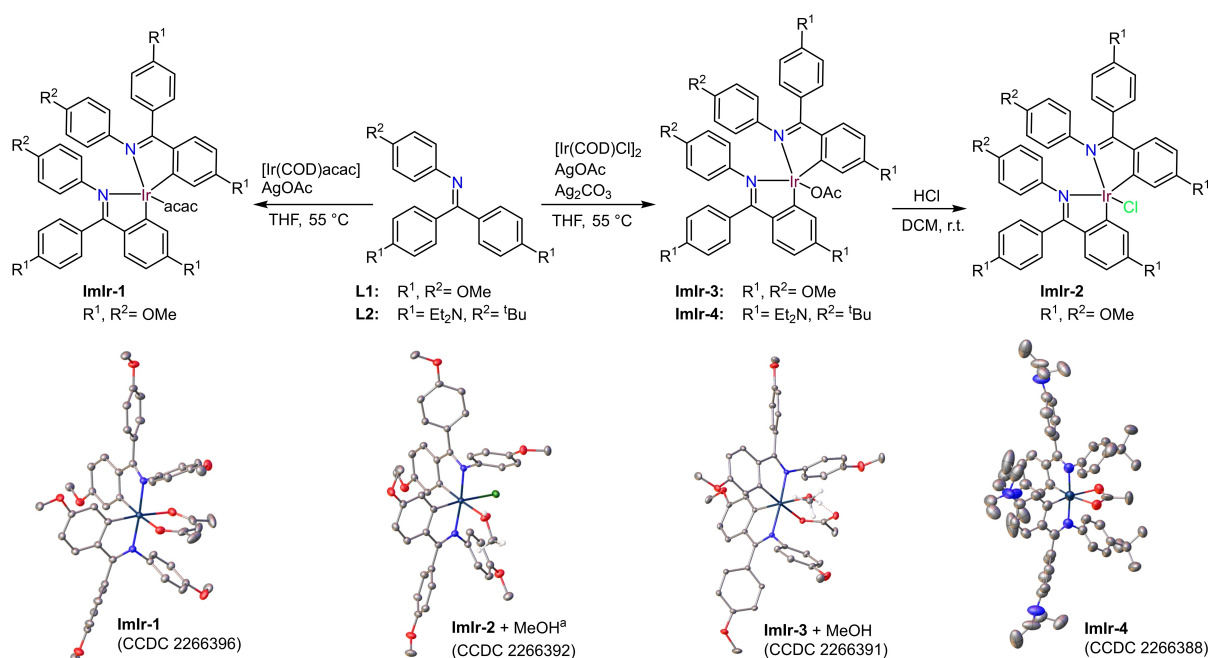
While the imine motif had already shown its potential as C,N ligand for various iridium catalyzed transformations^[20] its use for C–H activation remains to be demonstrated.

Therefore, a library of different imines was prepared. In a preliminary work, the potential of these ligands was evaluated in Ir-catalyzed direct borylation of amide **1a** via high-throughput (HT) screening (see SI for the full list of screened ligands). All screened C,N ligands exhibited excellent *ortho*-selectivity (*meta* and *para* products were not detected), albeit with modest yields. Triaryl imines with electron-donating substituents (Scheme 1, **L1**, **L2**) featured the highest

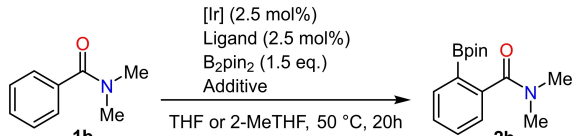
reactivities and were thus retained for the further study, i. e., the synthesis and isolation of the corresponding iridacycles.

While no complex formation was observed in the reaction between [Ir(COD)OMe]₂ and **L1/L2**, the reaction between [Ir(COD)Cl]₂ and **L1/L2** occurred smoothly in the presence of AgOAc. Remarkably, instead of the formation of the expected mono-cyclometallated species, two ligands coordinate to the metal center, furnishing bis-cyclometallated complexes – **ImIr** (Scheme 1). Reaction using NaOAc as base was notably slower highlighting the role of the AgOAc as halide abstractor and oxidant (See SI Table S12 for details). IrCl₃ could also be used as the metal precursor, but it proved to be impractical, due to very long reaction time and its incompatibility with ligand **L2** (see SI Table S12). The effect of auxiliary ligands was examined by performing ion-exchange while treating **ImIr-3** with anhydrous HCl, furnishing **ImIr-2**. The structures of all the synthesized complexes were confirmed via single-crystal X-ray analysis. Recrystallization from MeOH lead to its incorporation in the crystal structures of **ImIr-2** and **ImIr-3**. However, for catalysis all material was extensively dried and checked by NMR.

Subsequently, the catalytic activity of the **ImIr** complexes was evaluated in the direct borylation of **1b** (Table 1) and compared to *in situ* generated complexes (Entries 2–4), while good catalytic reactivity was observed with **ImIr-3** and **ImIr-4** (Entries 7–10). **ImIr-4** outcompeted **ImIr-3** (Entries 8–10) furnishing



Scheme 1. Iridium bis-cyclometallated complex synthesis. Thermal ellipsoids are drawn at the 50% probability level, and hydrogen atoms are omitted for clarity (except for solvent molecules). ^[a] Solvent disorder removed for clarity.

Table 1. Reaction optimization using **ImIr** precatalysts.


Entry	[Ir]	Ligand	Conv. %	Yield 2b , %
1	[Ir(COD)OMe] ₂	tmphe	100	0
2	[Ir(COD)OMe] ₂	L2	45	45
3	[Ir(COD)OMe] ₂ + 2.5 mol% HBpin	L2	53	53
4 ^[a]	[Ir(COD)OMe] ₂ + 150 mol% HBpin	L2	29	26
5	ImIr-2	-	0	0
6	ImIr-3	-	1	1
7 ^[b]	ImIr-3	-	68	68
8	ImIr-4	-	65	65
9	ImIr-4 + 2.5 mol% HBpin	-	81	81 (69%) ^[c]
10 ^[d]	ImIr-4 + 2.5 mol% HBpin	-	80	80
11 ^[d]	[Ir(COD)OMe] ₂	(C,N) ^[19]	19	19
12 ^[d]	[Ir(COD)OMe] ₂	(N,N) ^[11b]	72	57

Reaction conditions: **1b** (0.20 mmol, 1.0 eq.), yield was determined by ¹H NMR using 1,3,5-trimethoxybenzene as internal standard.

^[a] no B₂pin₂ was added,

^[b] **ImIr-3** (0.01 mmol, 5 mol%), 70 °C.

^[c] Isolated yield after repeating the reaction on 0.5 mmol scale.

^[d] MeTHF used as solvent.

2b in high yield at the temperature as low as 50 °C. The choice of the monodentate anionic ligand proved also to be critical as illustrated by the lack of reactivity of **ImIr-1** and **ImIr-2**, containing respectively acac

and Cl ions (Entry 5, for full data see SI Table S5). The high affinity of iridium towards halogens could be the reason why **ImIr-2** complex failed to deliver any product,^[20a] as during reaction scope we observed similar inhibition effect if starting material was contaminated with halogens.

The reaction efficiency could be further improved by the addition of catalytic amounts of HBpin (Entry 9, 10), as previously demonstrated for various iridium catalyzed systems.^[7d,11g,13a,22] The effect of HBpin was most pronounced for the precatalyst system compared to the *in situ* system (Entries 3,9). While changing the reaction medium to more sustainable MeTHF, no significant impact on the reaction outcome was observed with **ImIr-4** (Entry 10). However, the previously reported catalytic systems by Chattopadhyay^[19] and Mascareñas^[11b] exhibited lower conversions under these reaction conditions (Entries 11, 12) as the decreased temperature and the use of MeTHF seem to affect the reactivity and or selectivity of such *in situ* formed systems. Of note is that all studied complexes showed excellent air stability, with no decrease in the reactivity of **ImIr-4** even after 6 months of storage under air at room temperature.

Solvent Compatibility

Owing to the key advantages of the prepared iridacycle **ImIr-4**, such as high reactivity, stability, and solubility in various organic solvents, further optimization was performed via a high-throughput approach. The impact of various media, and in particular green solvents such as 2-MeTHF were investigated (Figure 2). **ImIr-4** exhibited better reactivity than its *in situ* counterpart ([Ir(COD)OMe]₂ with **L2**), while regioselectivity was independent of the solvent choice. The addition of

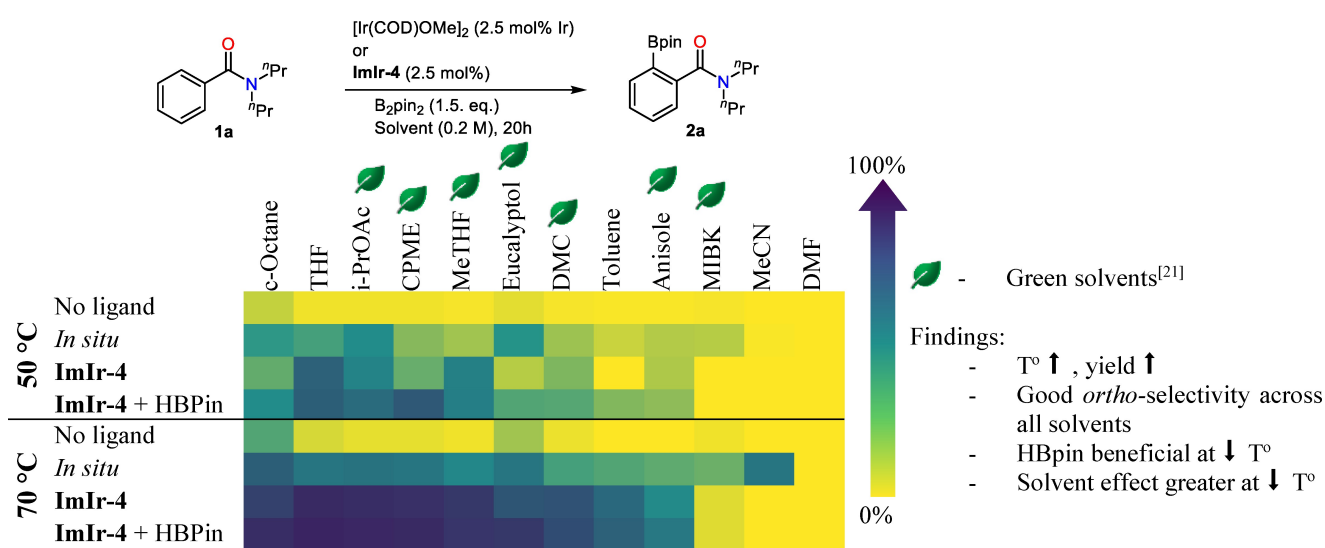


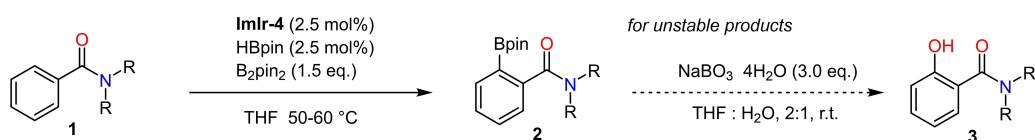
Figure 2. Reaction conditions: **1a** (0.10 mmol, 1.0 eq.). Yield was determined by quantitative GC FID.

HBpin improved the yield, but this effect was more prominent at lower temperatures (50 °C). Among the screened solvents, only strongly coordinating ones, such as methyl isobutyl ketone (MIBK), MeCN, and DMF, failed to produce any product.

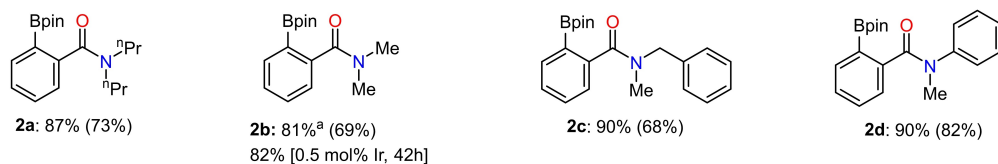
Substrate Scope: Amide Directed C–H Borylation of Arenes

With the optimized conditions in hand, the scope of the amide directed C–H borylation using **ImIr-4**/B₂pin₂/HBpin catalytic system was investigated (Scheme 2). We report the chemical yield of the products determined by a quantitative GC, or ¹H NMR analysis of the crude reaction mixture. Isolated yield was typically lower due to partial decomposition of the borylation products during purification (normal phase silica chromatography).^[7c,23] Rewardingly, under the standard reaction conditions, our catalytic system was compatible with various *N*-substituted amides (**1a–1d**), even at low catalyst loading of 0.5 mol% (**1b**).

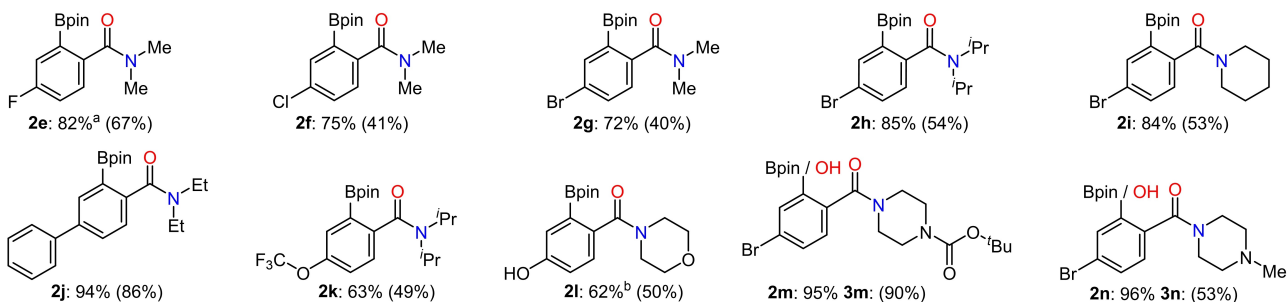
Different functional groups, including F-, Cl-, Br-, CF₃O-, HO- were well tolerated, furnishing the expected borylated products **2e–2i**, **2k**, **2m** in good yields. In all cases, exclusive *ortho*-selectivity was observed, even in the presence of multiple phenyl rings (**2c**, **2d**, **2j**, **2t**) thus demonstrating the high selectivity of the method. Piperazine derivatives **1m** and **1n** underwent the reaction smoothly, although a final oxidation step was required for proper isolation of the products (significant degradation of the borylated products on silica was observed). The phenol substrate **1l** underwent the desired C–H borylation after *in situ* protection using HBpin.^[24] In the case of *meta*-substituted benzamides, the reaction occurs selectively at the most sterically accessible position (**2o–2r**). Our catalytic system tolerates also more sterically encumbering amide DGs (**2s**, **2t**) although extended reaction time was necessary to reach high conversions.



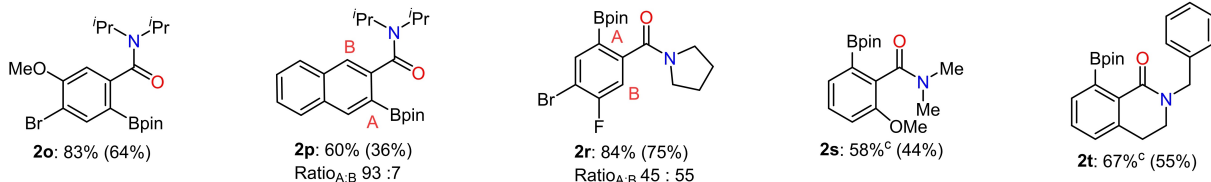
Scope for unsubstituted amides



Functional group scope



Ortho and meta substituted amide scope



Scheme 2. *Ortho*-selective C–H borylation of benzamides. **1** (0.50 mmol), yield determined by ¹H NMR using 1,3,5-trimethoxybenzene as internal standard, isolated yield given in parenthesis. Unless stated otherwise no other regioisomer could be detected. ^[a] Yield determined by quantitative GC/FID analysis; ^[b] Starting material was premixed with HBpin (0.55 mmol, 1.1 eq.) for 10 min before adding catalyst. ^[c] 62 h.

Substrate Scope: HT Screening Guided C–H Borylation of Arenes Bearing Multiple Directing Groups

To investigate the compatibility of our method with other directing groups and to assess its selectivity in complex substrates bearing several functional groups, HT screening of various phenyl-derivatives was conducted under slightly modified reaction conditions. A panel of 30 substrates was thus tested under 3 reaction conditions: 1) ligand-free conditions to study inherent reactivity of the substrates,^[22,25] 2) tetramethyl phenanthroline (tmphe) ligand: to promote formation and identification of *meta* and *para* products, 3) our standard conditions using **ImIr-4**. The results were rapidly analyzed using GC FID analysis.

Following the HT screening, the directing groups may be classified into 3 categories (Figure 3) based on their performance: 1) excellent directing groups (yielding over 75% conversion, dark blue); 2) average directing (yielding over 40% conversion, green); 3) poor directing groups (yielding below 15% conversion, yellow).

The results show significant differences between the explored substrates, with amides and ketones exhibiting the best reactivity (for the full list of screened compounds see SI Tables S8–S10). Notably, we hypothesized that some of the poor directing groups might work as inhibitors as we were unable to functionalize a benzamide substrate containing a -NO₂ group (see SI page S95). Additionally, strong Lewis

bases such as unhindered pyridines and phosphines can act as inhibitors in the reaction (see SI Table S7). Overall, this approach allowed rapid assessment of the selectivity and compatibility of a wide range of directing groups.

The viability of the results obtained through HT screening approach was confirmed by comparison with larger-scale reactions conducted in batch. Both, the *ortho*-selectivity, and the general reactivity trends could thus be validated (Scheme 3). Ketones **4a** and **4e** provided good isolated yields, while in the case of **4g**, direct derivatization via Suzuki coupling^[1b,11i,26] was necessary due to the low stability of the borylated compound. The corresponding product **6g** could thus be isolated in the synthetically useful yield, showcasing the possibility of telescoping further reaction steps without isolating the unstable boronic ester. Secondary benzamide **5f** was obtained in good yield, while sterically more accessible ⁿBu-substituted substrate **5i** and primary amide **5g** failed to produce any product (full list of failed substrates SI page 89). This hindrance-sensitivity of our catalyst shows its complementarity to the existing catalytic systems, for which the size of the amide group had virtually no effect on conversion.^[11c]

Finally, we focused our attention on substrates containing multiple directing groups (Scheme 4). Competition between amide and ester directing groups showed excellent selectivity for the amide-directed product (**8a** and **8b**). Similar results were obtained while using a substrate bearing both, ketone and ester

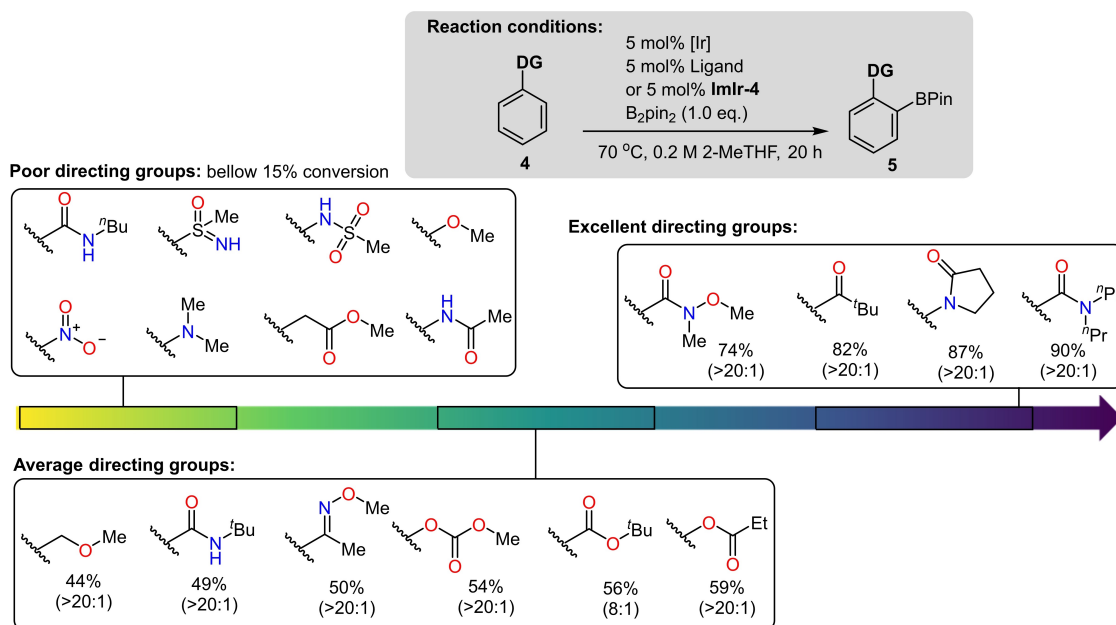
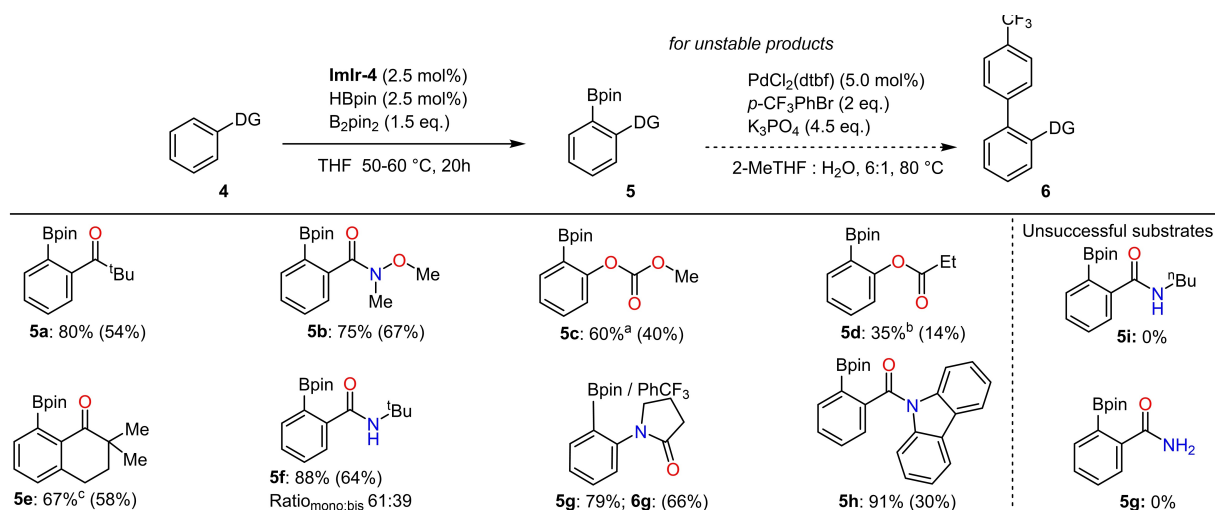
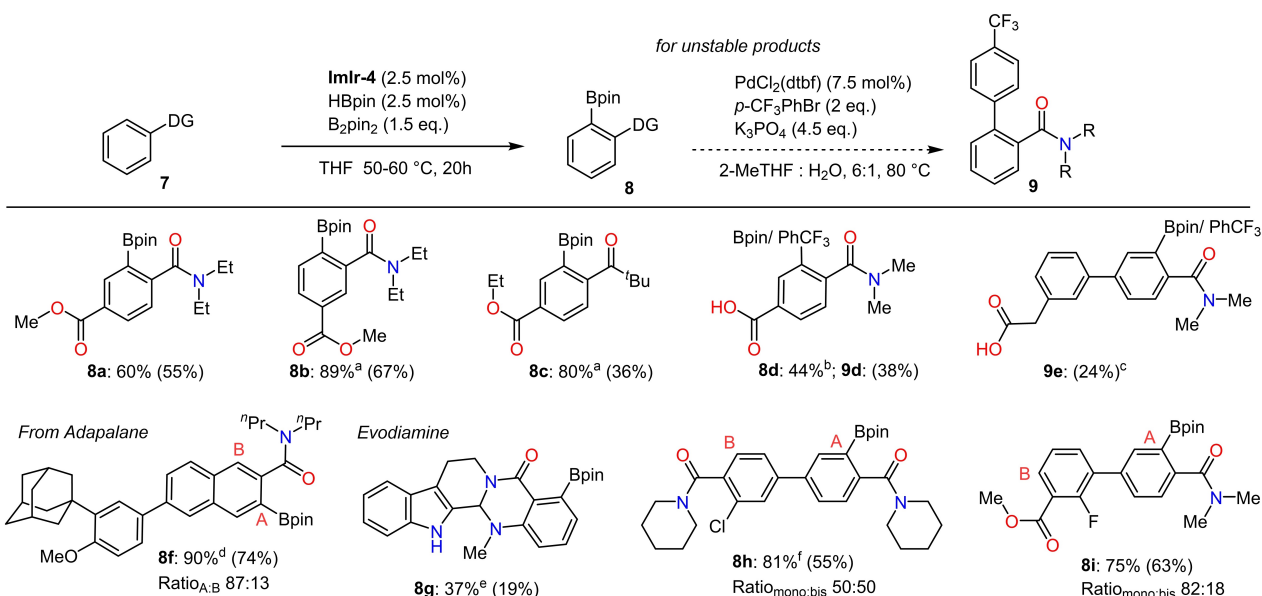


Figure 3. DG compatibility mapping using HT screening. Reaction conditions: reactions were carried out in 96 well Paradox plates, **4** (0.08 mmol), Conversions of starting materials given, *ortho* : (*meta* + *para*) selectivity in brackets, see Supporting information for details.



Scheme 3. Scope for different directing groups. Yield determined by ¹H NMR using 1,3,5-trimethoxybenzene as internal standard, isolated yield given in parenthesis. ^[a] **ImIr-4** (0.025 mmol, 5 mol%), B₂pin₂ (0.60 mmol, 1.2 eq.), cyclooctane, 85 °C. ^[b] **ImIr-4** (0.025 mmol, 5 mol%). ^[c] 62 h. ^[d] **ImIr-4** (0.025 mmol, 5 mol%), 2-MeTHF, 70 °C.



Scheme 4. Competition between multiple directing groups. Yield determined by ¹H NMR using 1,3,5-trimethoxybenzene as internal standard, isolated yield given in parenthesis. ^[a] 62 h. ^[b] HBpin 0.55 mmol (1.1 eq.), 62 h. ^[c] **ImIr-4** (0.025 mmol, 5 mol%), HBpin 0.55 mmol (1.1 eq.), THF (0.15 M), 62 h. ^[d] **ImIr-4** (0.025 mmol, 5 mol%). ^[e] **ImIr-4** (0.025 mmol, 5 mol%), THF (0.17 M), 80 °C, 62 h. ^[f] B₂Pin₂ (0.55 mmol, 1.1 eq.).

directing groups (**7c**). We observed that the presence of electron-withdrawing groups on substrates **7a–7d** generally translates into the need of extended reaction time compared to their analogues (**1a**, **1b**, **4a**). Notably, the method tolerates free carboxylic acids (**7d**, **7e**), after *in situ* protection using HBpin. In the case of the substrate **7e**, the reaction provided a single product **9e**, but the isolated yield was rather low probably due to the low stability of **8e**.

To the best of our knowledge, these are the first examples of selective directed C–H borylation in the presence of free carboxylic acid moiety. This is particularly interesting given that carboxylic groups have been used as a DG in a variety of C–H activation reactions,^[27] thus opening alternative possibilities for accessing multiple sites in complex molecules. We were pleased to see that drug-derived amide **8f** was isolated in excellent yield, while the borylation of natural product Evodiamine gave a modest yield (**8g**).

While substrates **7h**, **7i** bearing two similar coordinating motifs, delivered a mixture of mono and bis-borylated products.

Substrate Scope: C–H Borylation of Heterocycles and Nonaromatic C–H Borylation

Subsequently, we have challenged our catalytic system with more complex substrates going beyond simple aromatic systems (Scheme 5). Chattopadhyay has previously reported that in heterocyclic systems the DG effect is generally overruled by the inherent substrate reactivity,^[19] whereas Mascareñas reported successful directed borylation in five-membered heterocycles.^[11b] We discovered that while our method provided high yield for C–H borylation of amido-pyridine substrates, the regioselectivity changed significantly while modifying the steric effect of the amide (**11a**, **11b**). Previous study by Steel on pyridine borylation have highlighted that the interaction of the pyridine lone pair and iridium could lead to catalyst

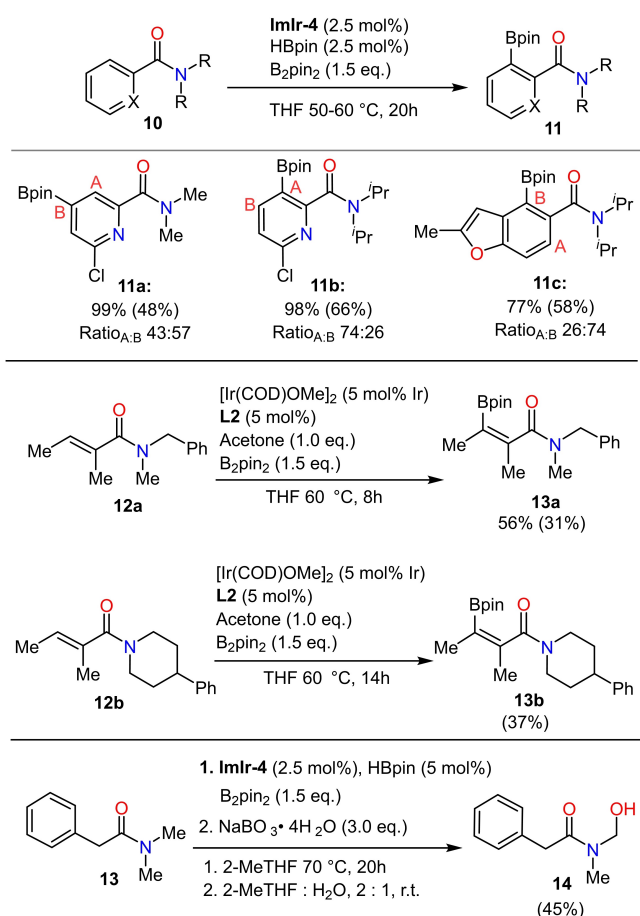
inhibition,^[28] which was strongly affected by substituents in 2-position of the pyridine.

Acrylamides (**12a** and **12b**) underwent the directed borylation albeit in modest yields. Undesired hydroboration side reaction could be partially avoided by introducing acetone as HBpin scavenger (see SI pages S88–S89). Previously Smith had reported an example on C–H borylation of enamines,^[8d] but to the best of our knowledge, products **13a**, **13b** represent the first example of C–H borylation of acrylamides. Finally, **ImIr-4** also promotes C(*sp*³)–H borylation, as exemplified on the substrate **13**,^[29] after oxidation of the crude mixture, product **14** was isolated.

Mechanistic Studies

To understand the reaction mechanism of cyclometalated **ImIr** complexes two main questions need to be answered. First, how HBpin helps to activate the system? Second, what is the active catalyst?

We started the mechanistic investigations by following the kinetic profile of the reaction using **ImIr-3** via *in situ* ¹H NMR experiments (Figure 4). Surprisingly a pronounced induction period was observed (approx. 60 min). In clear contrast, the *in situ* generated complex ([Ir(COD)OMe]₂ + **L1**) reacts immediately affording **2b** at an overall slower rate. This



Scheme 5. Borylation of heterocycles and nonaromatic substrates. **10** (0.50 mmol). Yield determined by ¹H NMR using 1,3,5-trimethoxybenzene as internal standard, isolated yield given in parenthesis.

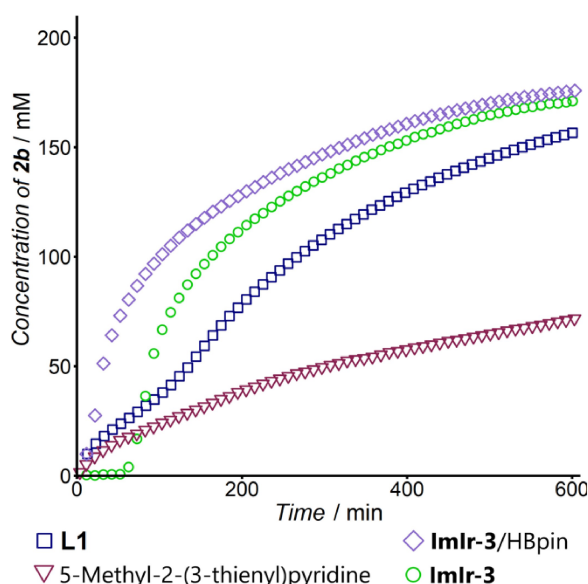
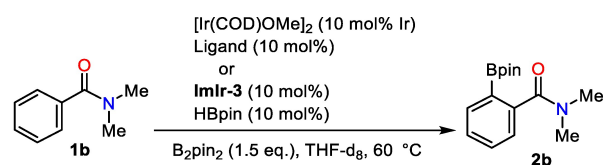


Figure 4. Kinetic study of the C–H borylation of benzamide **1b** using different catalytic systems.

observation supports our hypothesis that the complex **ImIr-3** works as a precatalyst and requires activation before entering the catalytic cycle.

Given that HBpin is generated stoichiometrically during the reaction and the described effects of HBpin in C–H borylation,^[11g,22,30] its role as the catalyst activator was surmised. As expected, addition of HBpin at the beginning of the reaction reconstituted high catalytic reactivity within the first minutes of the reaction. Importantly, a comparison study of the borylation of **1b** at 60 °C showed increased reactivity of the complex **ImIr-3** compared to the literature-known thienylpyridine ligand system.^[19]

During the kinetic experiments with **ImIr-3** (Figure 4, green circles), the formation of a distinct new species prior to the appearance of product **2b** was evidenced, which exhibited a new signal at –6.07 ppm (¹H NMR). Additionally, this intermediate would form immediately if HBpin was added at the beginning of the reaction (Figure 4, purple diamonds) and rapidly disappear at the start of product formation. The synthesis of this species could be reproduced by reacting the Ir-based precatalyst (**ImIr-3** or **ImIr-4**) with stoichiometric amounts of HBpin. The subsequently formed complex showed the same distinct wide signal at –6.07 ppm corresponding to 2H for complex **ImIr-3** (–6.13 ppm for **ImIr-4**), and the formation of Bpin-OAc could be detected.

In solution, in the presence of B₂pin₂ or HBpin, the intermediate **15** undergoes a further transformation into a complex mixture. By removing the excess B₂pin₂ and HBpin a crystalline material was obtained. After refining the data from the X-ray analysis, we managed to locate the hydride signals of complex **15** (Scheme 6). Attempts of dissolving the crystals in THF and quickly re-analyze them confirmed the presence of the hydride signals suggesting we did succeed in growing the crystals of the intermediate **15**. We also observed that the pure complex **15** starts to degrade in solution (at room temperature) releasing H₂, however this was not observed in kinetic studies. We therefore propose that during reaction complex **15** first reacts with B₂Pin₂, eliminating HBpin and forming a short lived intermediate **16** which rapidly enters the catalytic cycle (Scheme 6).

Furthermore, if complex **ImIr-3** was heated with only B₂pin₂ we observed a similar long induction time followed by quick formation of intermediate **15** and immediate conversion to a complex mixture (see SI pages S107–S110 for details). Following the addition of substrate **1a** to the mixture, the formation of product **2a** proceeded without an induction period.

Previous studies on C–H borylation using pincer ligand-containing iridium hydride complexes have found that boranes can form δ-borane, hydrogen bridged, or iridium-boron complexes.^[31] The structure of intermediate **15** is somewhat similar to the hydride

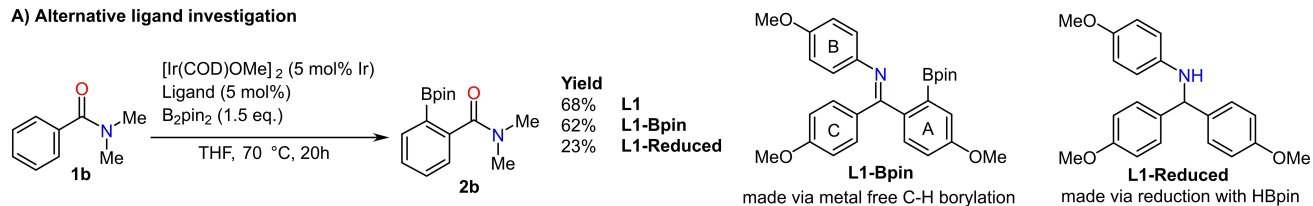
bridged complexes reported by Ozerov^[16a,31c] although their reactivity for C–H borylation differs significantly.

Since previous reports have highlighted both: activation^[32] and deactivation^[33] of the ligand by borylation, the possibility of *in situ* ligand borylation was explored (Scheme 6A). A separate experiment showed that borylation of **L1** using [Ir(COD)OMe]₂ (Scheme 6B) is sluggish, and only traces of the mono- and bis-borylated compounds were detected in HRMS.

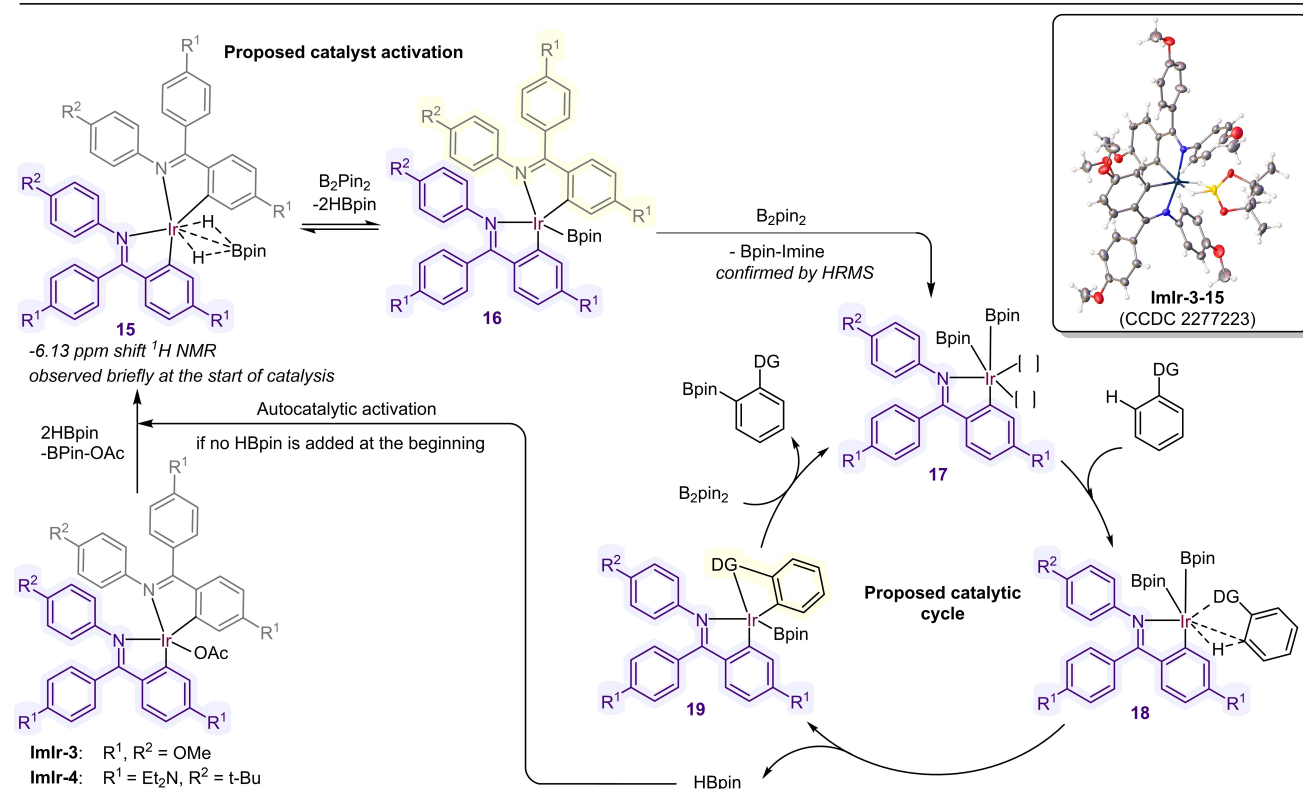
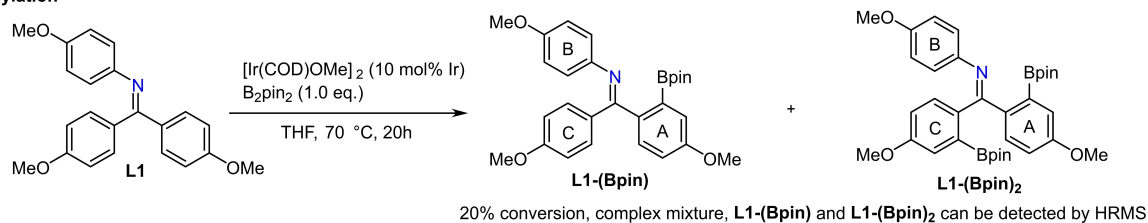
Additionally, we found the reactivity of the borylated ligand **L1-Bpin** is comparable to the non-functionalized **L1** (Scheme 6A). Therefore, it can be hypothesized that the borylated ligand is unlikely to be the key active ligand species since from the kinetics (Figure 4, blue squares) we clearly see that the reaction proceeds immediately if free ligand **L1** is used. While significantly lower reactivity was observed for reduced ligand **L1** (see SI page S110). This could also potentially explain the significant decrease of the reaction efficiency when HBpin was used as the only boron source (Table 1, Entry 4). Kinetic isotope studies revealed a low KIE value of 1.73 in an intermolecular competition experiment (**1b** + **1b-d₅**), with no significant H/D scrambling detected (see SI page 107). However, we observed no KIE in parallel reaction setup (**1b** vs **1b-d₅**, SI page 103). Based on this observation and following the literature known interpretation of the KIEs,^[34] C–H activation is expected to be the non rate-determining step and point towards more complex mechanism.^[11g,35] Further research in-depth kinetic studies^[36] may be needed to confirm these conclusions.

Based on our findings and the previously reported mechanisms^[7d,19] we propose the following catalytic cycle depicted in Scheme 6. First, the **ImIr** precatalyst undergoes activation either by reaction with HBpin forming complex **15** or by slow reaction with B₂pin₂. Complex **15** can then react further with B₂pin₂, forming **16**. Another reaction with B₂pin₂ eliminates borylated-imine ligand (see SI page S103) forming the proposed active catalyst **17**. Subsequently, an arene enters the cycle by coordinating to the complex **17** allowing for the C–H bond activation (**18**). Next HBpin is eliminated either through stepwise oxidative addition - reductive elimination^[7d] or through sigma bond metathesis^[37] forming intermediate **19**. Intermediate **19** can subsequently react with B₂pin₂ furnishing the borylated product, HBpin and closing the catalytic cycle. The proposed inner sphere mechanism via the key bis-cyclometallated species **19** is supported by the exceptionally high *ortho*-product selectivity and the observations that (during catalyst activation) **L1-(Bpin)** was generated from the bis-cyclometallated precursor. The induction period previously observed in the kinetic studies can be explained by catalyst activation from slow reaction with B₂pin₂ (see SI pages 100–103) followed by autocatalytic activation as soon

A) Alternative ligand investigation



B) Ligand borylation



Scheme 6. Mechanistic experiments and proposed reaction mechanism.

as HBpin is started to be produced.^[38] The presence of bis-cyclometallated active species has also been proposed previously for different C–H activation reactions.^[16c,39] Additionally, the lack of significant kinetic isotope effect, which is contrary to the undirected borylation^[7d] further supports the differences in reaction mechanism.

Conclusion

In conclusion, we have developed a method for *ortho*-selective C–H borylation using stable bis-cyclometal-

lated iridium complexes. Utilizing high-throughput screening of different C,N ligands, triaryl imines were identified as the most reactive ligands. Notably, these ligands enabled the formation of bis-cyclometallated iridium complexes in a straightforward, single-step reaction. The synthesized bis-cyclometallated iridium complexes, outperformed the corresponding *in situ* formed counterpart and displayed consistent regioselectivity across a wide range of solvents, including environmentally friendly mediums. Substrate scope studies demonstrated the application of our method for amide-directed C–H borylation, showcasing its selec-

tivity and tolerance towards various functional groups. Moreover, high-throughput screening allowed rapid evaluation of the reactivity of different directing groups, enabling us to systematically predict the functionalization of substrates featuring multiple directing groups. Mechanistic investigations suggest the bis-cyclometallated iridium complex first undergoes activation with HBpin followed by subsequent elimination of one of the cyclometallated imines. As the catalyst structure allows for easy modifications future research directions could include fine-tuning it for different directing groups and more detailed mechanistic studies, understanding of reaction rates for different substrate classes. Overall, we believe that our developed methodology holds promise for automated late-stage functionalization of complex molecules, simplifying the diversification and preparation of novel bioactive molecules.

Experimental Section

All the chemicals and reagents were purchased and used as received, unless noted otherwise. All reactions were performed with the exclusion of air and moisture, under an inert atmosphere of nitrogen or argon with magnetic stirring, unless noted otherwise. All solvents were dried over 3 Å or 4 Å molecular sieves prior to use. Column chromatographic purifications were performed on a CombiFlash Nextgen 300+ with pre-packed Chromabond® SiO₂ columns (40–63 µm) using a mobile phase indicated. Preparative supercritical fluid chromatography (SFC) was performed using Waters Acquity UPC²/QDa equipped with PDA Detector and Waters Torus columns. NMR spectra were recorded on a Bruker Avance operating for ¹H NMR at 400 Neo 400 MHz spectrometer or Bruker AVANCE Neo 600 MHz spectrometer. The High-Resolution Mass Spectrometry (HRMS) analyses were performed on Q Exactive Orbitrap Mass Spectrometer (Thermo Fisher Scientific). The X-ray crystal structure was obtained with Bruker D8 VENTURE dual wavelength Mo/Ag four-circle diffractometer or Rigaku Oxford Diffraction Supernova diffractometer.

General Procedure (Ortho-Borylation of 1b)

Biotage® MW vial was charged with *N,N*-dimethylbenzamide **1b** (73.4 mg, 0.5 mmol, 1.0 eq.) and B₂pin₂ (190 mg, 0.75 mmol, 1.5 eq.) and transferred to argon filled glovebox. Afterwards **ImIr-4** (14.5 mg, 0.0125 mmol, 0.025 eq.) was added as a stock solution in THF (0.02 M) followed by a stock solution of HBpin (6.6 mg, 0.0125 mmol, 0.025 eq.) in THF (0.1665 M). Lastly THF (1.80 mL) was added, the vial was briefly stirred, sealed, taken out of the glovebox, and left to stir at 50 °C for 20 h. Afterwards the vial was cooled, opened and 1,2,4,5-tetramethyl benzene was added as internal standard. A sample was taken, and crude yield was determined by quantitative GC/FID. For samples analyzed by NMR 1,3,5-trimethoxybenzene was used instead. Afterwards the mixture was concentrated under reduced pressure and purified by column chromatography to afford product **2b**.

Crystal structures are available free of charge on The Cambridge Crystallographic Data Centre via www.ccdc.cam.ac.uk/ structures with the following numbers: **ImIr-1** (CCDC 2266396), **ImIr-2** (CCDC 2266392), **ImIr-3** (CCDC 2266391), **ImIr-4** (CCDC 2266388), **ImIr-3–15** (CCDC 2277223).

Acknowledgements

We thank Dr. Christopher Golz (Göttingen University) and Dr. M. G. Montgomery (Syngenta) for the X-ray crystallographic analysis. We are grateful to the analytical and separation departments at Syngenta AG, namely Katharina Gaus, Thomas Stadelmann and Sidney Behringer for their help with NMR studies and purification of difficult substrates and Abdallah Sandhu for the preparation of some of the starting materials. Lastly, we would like to thank Dr. Simon Williams, Dr. Daria Grosheva and Dr. Andrei Iosub for fruitful discussions. We thank the European Union H2020 research and innovation program under the Marie S. Curie Grant Agreement no. 860762 (MSCA ITN: CHAIR) for the extensive funding.

References

- [1] a) T. Dalton, T. Faber, F. Glorius, *ACS Cent. Sci.* **2021**, *7*, 245–261; b) A. J. Lyons, A. Clarke, H. Fisk, B. Jackson, P. R. Moore, S. Oke, T. O. Ronson, R. E. Meadows, *Org. Process Res. Dev.* **2022**, *26*, 1378–1388; c) R. N. Bream, H. Clark, D. Edney, A. Harsanyi, J. Hayler, A. Ironmonger, N. Mc Cleary, N. Phillips, C. Priestley, A. Roberts, P. Rushworth, P. Szeto, M. R. Webb, K. Wheelhouse, *Org. Process Res. Dev.* **2021**, *25*, 529–540.
- [2] a) I. A. Mkhaliid, J. H. Barnard, T. B. Marder, J. M. Murphy, J. F. Hartwig, *Chem. Rev.* **2010**, *110*, 890–931; b) S. Darses, J. P. Genet, *Chem. Rev.* **2008**, *108*, 288–325; c) R. Bisht, C. Haldar, M. M. M. Hassan, M. E. Hoque, J. Chaturvedi, B. Chattopadhyay, *Chem. Soc. Rev.* **2022**, *51*, 5042–5100.
- [3] a) J. Wen, D. Wang, J. Qian, D. Wang, C. Zhu, Y. Zhao, Z. Shi, *Angew. Chem. Int. Ed. Engl.* **2019**, *58*, 2078–2082; b) W. Miura, K. Hirano, M. Miura, *Org. Lett.* **2016**, *18*, 3742–3745.
- [4] a) J. V. Obligacion, S. P. Semproni, P. J. Chirik, *J. Am. Chem. Soc.* **2014**, *136*, 4133–4136; b) J. V. Obligacion, P. J. Chirik, *ACS Catal.* **2017**, *7*, 4366–4371; c) P. Ghosh, R. Schoch, M. Bauer, A. Jacobi von Wangelin, *Angew. Chem. Int. Ed. Engl.* **2022**, *61*, e202110821.
- [5] S. Sarkar, N. Y. Kumar, L. Ackermann, *Chemistry* **2017**, *23*, 84–87.
- [6] a) S. M. Preshlock, B. Ghaffari, P. E. Maligres, S. W. Krska, R. E. Maleczka Jr., M. R. Smith, 3rd, *J. Am. Chem. Soc.* **2013**, *135*, 7572–7582; b) J. S. Wright, P. J. H. Scott, P. G. Steel, *Angew. Chem. Int. Ed. Engl.* **2021**, *60*, 2796–2821; c) M. M. M. Hassan, S. Guria, S. Dey, J. Das, B. Chattopadhyay, *Sci. Adv.* **2023**, *9*, eadg3311.
- [7] a) J. Y. Cho, M. K. Tse, D. Holmes, R. E. Maleczka Jr., M. R. Smith, 3rd, *Science* **2002**, *295*, 305–308; b) T.

- Ishiyama, J. Takagi, K. Ishida, N. Miyaura, N. R. Anastasi, J. F. Hartwig, *J. Am. Chem. Soc.* **2002**, *124*, 390–391; c) T. Ishiyama, J. Takagi, J. F. Hartwig, N. Miyaura, *Angew. Chem. Int. Ed. Engl.* **2002**, *41*, 3056–3058; d) T. M. Boller, J. M. Murphy, M. Hapke, T. Ishiyama, N. Miyaura, J. F. Hartwig, *J. Am. Chem. Soc.* **2005**, *127*, 14263–14278; e) M. A. Larsen, J. F. Hartwig, *J. Am. Chem. Soc.* **2014**, *136*, 4287–4299; f) S. Rej, N. Chatani, *J. Am. Chem. Soc.* **2021**, *143*, 2920–2929; g) C. N. Iverson, M. R. Smith, *J. Am. Chem. Soc.* **1999**, *121*, 7696–7697; h) J.-Y. Cho, C. N. Iverson, M. R. Smith, *J. Am. Chem. Soc.* **2000**, *122*, 12868–12869.
- [8] a) A. Ros, R. Fernandez, J. M. Lassaletta, *Chem. Soc. Rev.* **2014**, *43*, 3229–3243; b) L. Xu, G. Wang, S. Zhang, H. Wang, L. Wang, L. Liu, J. Jiao, P. Li, *Tetrahedron* **2017**, *73*, 7123–7157; c) M. R. Smith, 3rd, R. Bisht, C. Haldar, G. Pandey, J. E. Dannatt, B. Ghaffari, R. E. Maleczka, Jr., B. Chattopadhyay, *ACS Catal.* **2018**, *8*, 6216–6223; d) P. C. Roosen, V. A. Kallepalli, B. Chattopadhyay, D. A. Singleton, R. E. Maleczka Jr., M. R. Smith, 3rd, *J. Am. Chem. Soc.* **2012**, *134*, 11350–11353.
- [9] T. A. Boebel, J. F. Hartwig, *J. Am. Chem. Soc.* **2008**, *130*, 7534–7535.
- [10] a) S. Kawamorita, H. Ohmiya, K. Hara, A. Fukuoka, M. Sawamura, *J. Am. Chem. Soc.* **2009**, *131*, 5058–5059; b) T. Ishiyama, H. Isou, T. Kikuchi, N. Miyaura, *Chem. Commun.* **2010**, *46*, 159–161; c) B. Ghaffari, S. M. Preshlock, D. L. Plattner, R. J. Staples, P. E. Maligres, S. W. Krska, R. E. Maleczka Jr., M. R. Smith, 3rd, *J. Am. Chem. Soc.* **2014**, *136*, 14345–14348; d) J. Jiao, W. Nie, P. Song, P. Li, *Org. Biomol. Chem.* **2020**, *19*, 355–359.
- [11] a) H. L. Li, Y. Kuninobu, M. Kanai, *Angew. Chem. Int. Ed. Engl.* **2017**, *56*, 1495–1499; b) D. Marcos-Atanes, C. Vidal, C. D. Navo, F. Peccati, G. Jimenez-Oses, J. L. Mascarenas, *Angew. Chem. Int. Ed. Engl.* **2023**, *62*, e202214510; c) S. T. Bai, C. B. Bheeter, J. N. H. Reek, *Angew. Chem. Int. Ed. Engl.* **2019**, *58*, 13039–13043; d) A. Ros, B. Estepa, R. Lopez-Rodriguez, E. Alvarez, R. Fernandez, J. M. Lassaletta, *Angew. Chem. Int. Ed. Engl.* **2011**, *50*, 11724–11728; e) A. J. Roering, L. V. Hale, P. A. Squier, M. A. Ringgold, E. R. Wiederspan, T. B. Clark, *Org. Lett.* **2012**, *14*, 3558–3561; f) L. V. A. Hale, K. A. McGarry, M. A. Ringgold, T. B. Clark, *Organometallics* **2015**, *34*, 51–55; g) N. Le, N. L. Chuang, C. M. Oliver, A. V. Samoshin, J. T. Hemphill, K. C. Morris, S. N. Hyland, H. Guan, C. E. Webster, T. B. Clark, *ACS Catal.* **2023**, *13*, 12877–12893; h) R. Lopez-Rodriguez, A. Ros, R. Fernandez, J. M. Lassaletta, *J. Org. Chem.* **2012**, *77*, 9915–9920; i) A. Ros, R. Lopez-Rodriguez, B. Estepa, E. Alvarez, R. Fernandez, J. M. Lassaletta, *J. Am. Chem. Soc.* **2012**, *134*, 4573–4576.
- [12] a) K. M. Crawford, T. R. Ramseyer, C. J. Daley, T. B. Clark, *Angew. Chem. Int. Ed. Engl.* **2014**, *53*, 7589–7593; b) B. Chattopadhyay, M. E. Hoque, M. M. M. Hassan, C. Haldar, S. Dey, S. Guria, J. Chaturvedi, *Synthesis* **2022**, *54*, 3328–3340.
- [13] a) E. D. Slack, T. J. Colacot, *Org. Lett.* **2021**, *23*, 1561–1565; b) C. C. C. J. Seechurn, V. Sivakumar, D. Satoskar, T. J. Colacot, *Organometallics* **2014**, *33*, 3514–3522.
- [14] a) M. A. Bennett, D. L. Milner, *J. Am. Chem. Soc.* **1969**, *91*, 6983–6994; b) A. C. Cope, R. W. Siekman, *J. Am. Chem. Soc.* **1965**, *87*, 3272–3273; c) R. G. Bergman, *Science* **1984**, *223*, 902–908; d) A. D. Ryabov, *Synthesis* **1985**, *1985*, 233–252; e) S. A. Bezman, P. H. Bird, A. R. Fraser, J. A. Osborn, *Inorg. Chem.* **2002**, *19*, 3755–3763; f) S. Attar, J. H. Nelson, J. Fischer, A. de Cian, J.-P. Sutter, M. Pfeffer, *Organometallics* **2002**, *14*, 4559–4569; g) T. R. Cook, P. J. Stang, *Chem. Rev.* **2015**, *115*, 7001–7045.
- [15] a) D. A. Colby, R. G. Bergman, J. A. Ellman, *Chem. Rev.* **2010**, *110*, 624–655; b) R. G. Bergman, *Nature* **2007**, *446*, 391–393; c) X. Chen, K. M. Engle, D. H. Wang, J. Q. Yu, *Angew. Chem. Int. Ed. Engl.* **2009**, *48*, 5094–5115; d) A. M. Messinis, J. C. A. Oliveira, A. C. Stückl, L. Ackermann, *ACS Catal.* **2022**, *12*, 4947–4960.
- [16] a) L. P. Press, A. J. Kosanovich, B. J. McCulloch, O. V. Ozerov, *J. Am. Chem. Soc.* **2016**, *138*, 9487–9497; b) P. Gandeepan, T. Muller, D. Zell, G. Cera, S. Warratz, L. Ackermann, *Chem. Rev.* **2019**, *119*, 2192–2452; c) N. Selander, B. Willy, K. J. Szabo, *Angew. Chem. Int. Ed. Engl.* **2010**, *49*, 4051–4053; d) L. Ackermann, R. Viceinte, H. K. Potukuchi, V. Pirovano, *Org. Lett.* **2010**, *12*, 5032–5035; e) M. Simonetti, D. M. Cannas, X. Just-Baringo, I. J. Vitorica-Yrezabal, I. Larrosa, *Nat. Chem.* **2018**, *10*, 724–731.
- [17] a) M. T. Findlay, P. Domingo-Legarda, G. McArthur, A. Yen, I. Larrosa, *Chem. Sci.* **2022**, *13*, 3335–3362; b) M. T. Findlay, A. S. Hogg, J. J. Douglas, I. Larrosa, *Green Chem.* **2023**, *25*, 2394–2400.
- [18] G. Wang, L. Liu, H. Wang, Y. S. Ding, J. Zhou, S. Mao, P. Li, *J. Am. Chem. Soc.* **2017**, *139*, 91–94.
- [19] M. E. Hoque, M. M. M. Hassan, B. Chattopadhyay, *J. Am. Chem. Soc.* **2021**, *143*, 5022–5037.
- [20] a) J. Mas-Rosello, T. Smejkal, N. Cramer, *Science* **2020**, *368*, 1098–1102; b) R. J. Li, C. Ling, W. R. Lv, W. Deng, Z. J. Yao, *Inorg. Chem.* **2021**, *60*, 5153–5162.
- [21] a) C. M. Alder, J. D. Hayler, R. K. Henderson, A. M. Redman, L. Shukla, L. E. Shuster, H. F. Sneddon, *Green Chem.* **2016**, *18*, 3879–3890; b) J. F. Campos, M.-C. Scherrmann, S. Berteina-Raboin, *Green Chem.* **2019**, *21*, 1531–1539; c) R. K. Henderson, C. Jiménez-González, D. J. C. Constable, S. R. Alston, G. G. A. Inglis, G. Fisher, J. Sherwood, S. P. Binks, A. D. Curzons, *Green Chem.* **2011**, *13*; d) F. P. Byrne, S. Jin, G. Paggiola, T. H. M. Petchey, J. H. Clark, T. J. Farmer, A. J. Hunt, C. Robert McElroy, J. Sherwood, *Sustain. Chem. Process.* **2016**, *4*.
- [22] M. M. M. Hassan, B. Mondal, S. Singh, C. Haldar, J. Chaturvedi, R. Bisht, R. B. Sunoj, B. Chattopadhyay, *J. Org. Chem.* **2022**, *87*, 4360–4375.
- [23] a) K. Yamazaki, S. Kawamorita, H. Ohmiya, M. Sawamura, *Org. Lett.* **2010**, *12*, 3978–3981; b) O. Kuleshova, S. Asako, L. Ilies, *ACS Catal.* **2021**, *11*, 5968–5973.

- [24] a) R. Oeschger, B. Su, I. Yu, C. Ehinger, E. Romero, S. He, J. Hartwig, *Science* **2020**, *368*, 736–741; b) I. F. Yu, J. L. Manske, A. Dieguez-Vazquez, A. Misale, A. E. Pashenko, P. K. Mykhailiuk, S. V. Ryabukhin, D. M. Volochnyuk, J. F. Hartwig, *Nat. Chem.* **2023**, *15*, 685–693.
- [25] a) S. Mao, B. Yuan, X. Wang, Y. Zhao, L. Wang, X. Y. Yang, Y. M. Chen, S. Q. Zhang, P. Li, *Org. Lett.* **2022**, *24*, 3594–3598; b) L. Liu, G. Wang, J. Jiao, P. Li, *Org. Lett.* **2017**, *19*, 6132–6135.
- [26] P. Gao, M. Szostak, *Org. Lett.* **2020**, *22*, 6010–6015.
- [27] a) S. D. Friis, M. J. Johansson, L. Ackermann, *Nat. Chem.* **2020**, *12*, 511–519; b) M. Font, J. M. Quibell, G. J. P. Perry, I. Larrosa, *Chem. Commun.* **2017**, *53*, 5584–5597; c) M. Pichette Drapeau, L. J. Goossen, *Chemistry* **2016**, *22*, 18654–18677.
- [28] S. A. Sadler, H. Tajuddin, I. A. Mkhaliid, A. S. Batsanov, D. Albesa-Jove, M. S. Cheung, A. C. Maxwell, L. Shukla, B. Roberts, D. C. Blakemore, Z. Lin, T. B. Marder, P. G. Steel, *Org. Biomol. Chem.* **2014**, *12*, 7318–7327.
- [29] a) M. Reille-Seroussi, P. Meyer-Ahrens, A. Aust, A. L. Feldberg, H. D. Mootz, *Angew. Chem. Int. Ed. Engl.* **2021**, *60*, 15972–15979; b) M. Royo, J. Alsina, E. Giralt, U. Slomczynska, F. Albericio, *J. Chem. Soc. Perkin Trans. 1* **1995**; c) J. E. Dannatt, A. Yadav, M. R. Smith, 3rd, R. E. Maleczka, Jr., *Tetrahedron* **2022**, *109*, 132578; d) S. N. Hyland, E. A. Meck, M. Tortosa, T. B. Clark, *Tetrahedron Lett.* **2019**, *60*, 1096–1098.
- [30] J. Trouvé, P. Rajeshwaran, M. Tomasini, A. Perennes, T. Roisnel, A. Poater, R. Gramage-Doria, *ACS Catal.* **2023**, *13*, 7715–7729.
- [31] a) M. A. Esteruelas, A. Martinez, M. Olivan, E. Onate, *Chemistry* **2020**, *26*, 12632–12644; b) T. J. Hebden, M. C. Denney, V. Pons, P. M. Piccoli, T. F. Koetzle, A. J. Schultz, W. Kaminsky, K. I. Goldberg, D. M. Heinekey, *J. Am. Chem. Soc.* **2008**, *130*, 10812–10820; c) W.-C. Shih, O. V. Ozerov, *Organometallics* **2016**, *36*, 228–233; d) N. Arnold, S. Mozo, U. Paul, U. Radius, H. Braunschweig, *Organometallics* **2015**, *34*, 5709–5715.
- [32] M. Zhang, H. Wu, J. Yang, G. Huang, *ACS Catal.* **2021**, *11*, 4833–4847.
- [33] R. J. Oeschger, M. A. Larsen, A. Bismuto, J. F. Hartwig, *J. Am. Chem. Soc.* **2019**, *141*, 16479–16485.
- [34] E. M. Simmons, J. F. Hartwig, *Angew. Chem. Int. Ed. Engl.* **2012**, *51*, 3066–3072.
- [35] a) T. P. Pabst, L. Quach, K. T. MacMillan, P. J. Chirik, *Chem* **2021**, *7*, 237–254; b) J. V. Obligacion, S. P. Semproni, I. Pappas, P. J. Chirik, *J. Am. Chem. Soc.* **2016**, *138*, 10645–10653; c) T. P. Pabst, J. V. Obligacion, E. Rochette, I. Pappas, P. J. Chirik, *J. Am. Chem. Soc.* **2019**, *141*, 15378–15389.
- [36] C. Alamillo-Ferrer, G. Hutchinson, J. Bures, *Nat Rev Chem* **2023**, *7*, 26–34.
- [37] a) K. M. Altus, J. A. Love, *Commun. Chem.* **2021**, *4*, 173; b) J. F. Hartwig, K. S. Cook, M. Hapke, C. D. Incarvito, Y. Fan, C. E. Webster, M. B. Hall, *J. Am. Chem. Soc.* **2005**, *127*, 2538–2552.
- [38] J. F. Hartwig, *Acc. Chem. Res.* **2012**, *45*, 864–873.
- [39] a) J. M. Zakis, T. Smejkal, J. Wencel-Delord, *Chem. Commun.* **2022**, *58*, 483–490; b) W. Li, S. Zhang, X. Feng, X. Yu, Y. Yamamoto, M. Bao, *Org. Lett.* **2021**, *23*, 2521–2526; c) K. Korvorapun, J. Struwe, R. Kuniyil, A. Zangarelli, A. Casnati, M. Waeterschoot, L. Ackermann, *Angew. Chem. Int. Ed. Engl.* **2020**, *59*, 18103–18109.
-